Design philosophies of magnetic current limiter and high temperature superconducting fault current limiter-A comparative study

メタデータ	言語: eng
	出版者:
	公開日: 2017-12-07
	キーワード (Ja):
	キーワード (En):
	作成者:
	メールアドレス:
	所属:
URL	https://doi.org/10.24517/00049229

DESIGN PHILOSOPHIES OF MAGNETIC CURRENT LIMITER AND HIGH TEMPERATURE SUPERCONDUCTING FAULT CURRENT LIMITER – A COMPARATIVE STUDY

S. C. Mukhopadhyay, M.Iwahara* and S.Yamada*
Institute of Information Sciences and Technology
Massey University, Private bag 11 222
Palmerston North, New Zealand
Email: S.C.Mukhopadhyay@massey.ac.nz

* Kanazawa University, Kanazawa, Japan

Abstract

In this paper the basic design philosophy of designing of two types of current limiter based on saturable core biased by permanent magnet and superconducting element has been described. The application areas of this type of devices are to be explored. The operating principle of permanent magnet based fault current limiter is the change of the magnetic state of the core. Under normal operation the core operates in saturation and it comes out of saturation once the fault or abnormal condition takes place. The inductance of the limiter changes from a low saturated value to a high unsaturated value and thus limits the fault current. The superconducting fault current limiter offers a negligible resistance during normal condition and the resistance value jumps to a high value during fault condition. Some simulation and experimental results have been presented.

1. INTRODUCTION

A large current flows during the fault, short-circuit or any other abnormal condition in power system. There is always a need to use some kind of external device to limit the peak value of the fault current. In this paper the operating principle of two types of fault current limiter has been described. A few experimental results and simulation results have been presented.

A magnetic current limiter is based on permanent magnet, saturable core and winding. The permanent magnet is used to bias the core and the core operates in saturation under normal operating condition. The winding carries the current of the system. Under normal operation the inductance offered by the limiter is negligible. During fault condition the large value of fault current forces the core to come out of saturation and go to unsaturated state. Thus there is a change of inductance and the large unsaturated inductance is used to limit the fault current.

On the other hand the fault current limiter based on superconducting material relies on the change of electrical properties of the superconducting wire. The wire possess very low resistance (ideally zero resistance)

during the normal state (i.e. the superconducitng state) and offers a very large resistance during the fault state and thereby limits the fault current.

2. MAGNETIC CURRENT LIMITER

The operating principle of magnetic current limiter (MCL) is explained with the help of Fig. 1. The permanent magnet is sandwiched between the saturable core and is used to saturate the core under normal operating condition. The direction of the magnetomotive force and the alternating current is additive in core#1 and subtractive in core#2 at the same time. During normal condition during which the operating current is low, both the cores are under saturation. So the effective impedance of the system is low. During fault, the large value of current forces the cores to come out of saturation in alternate half-cycle, so unsaturated inductance of one core in combination with the saturated inductance of the other core restricts the flow of abnormally large value of fault current. Fig. 2 shows the operating point of one core based on the B-H characteristics of the permanent magnet (PM) and core. In order to have saturation the core such as ferrite, should have a very low value of saturation flux density compared to PM. Fig. 3 shows the complete flux-current characteristics of both the core-PM assembly.
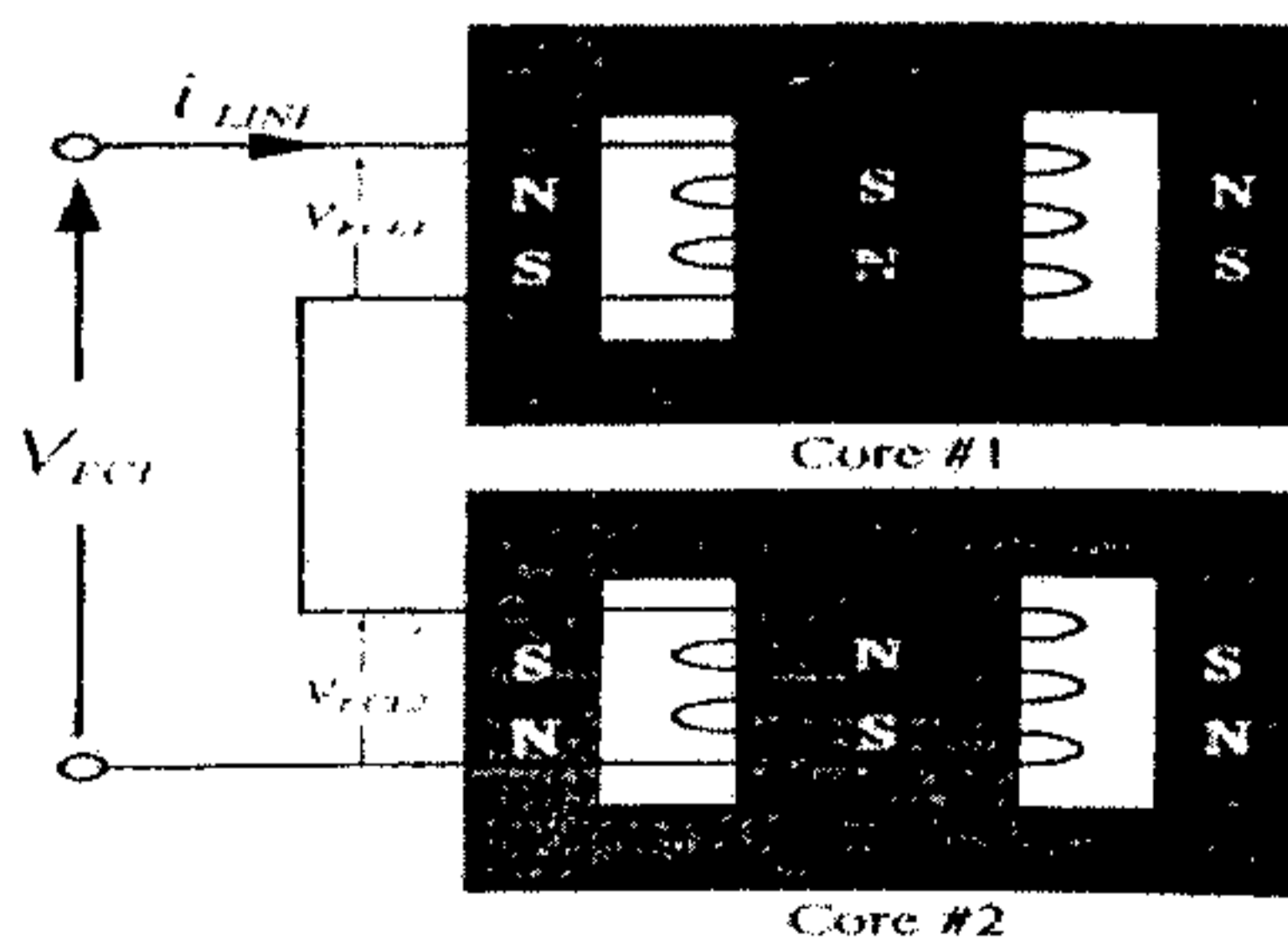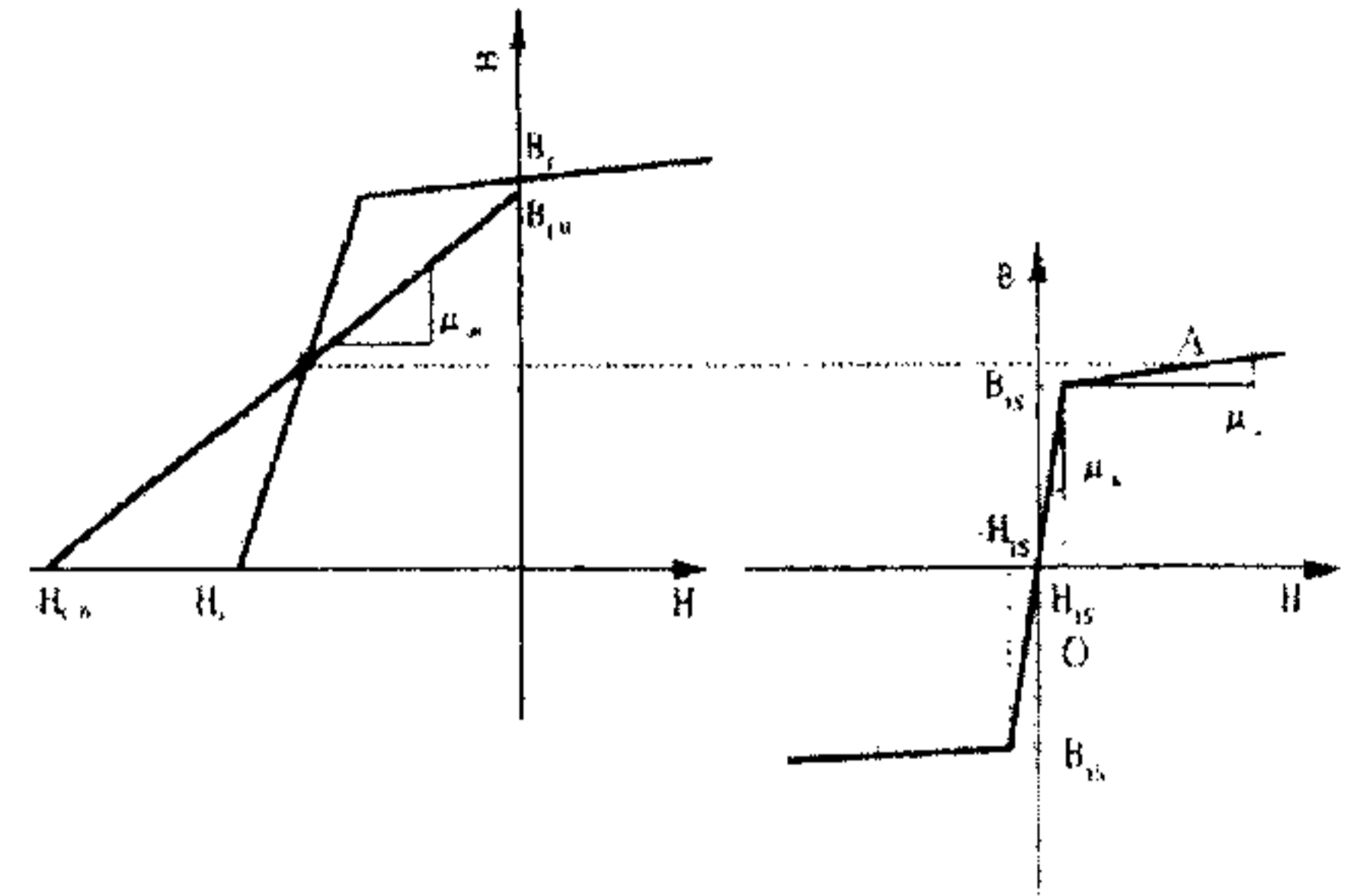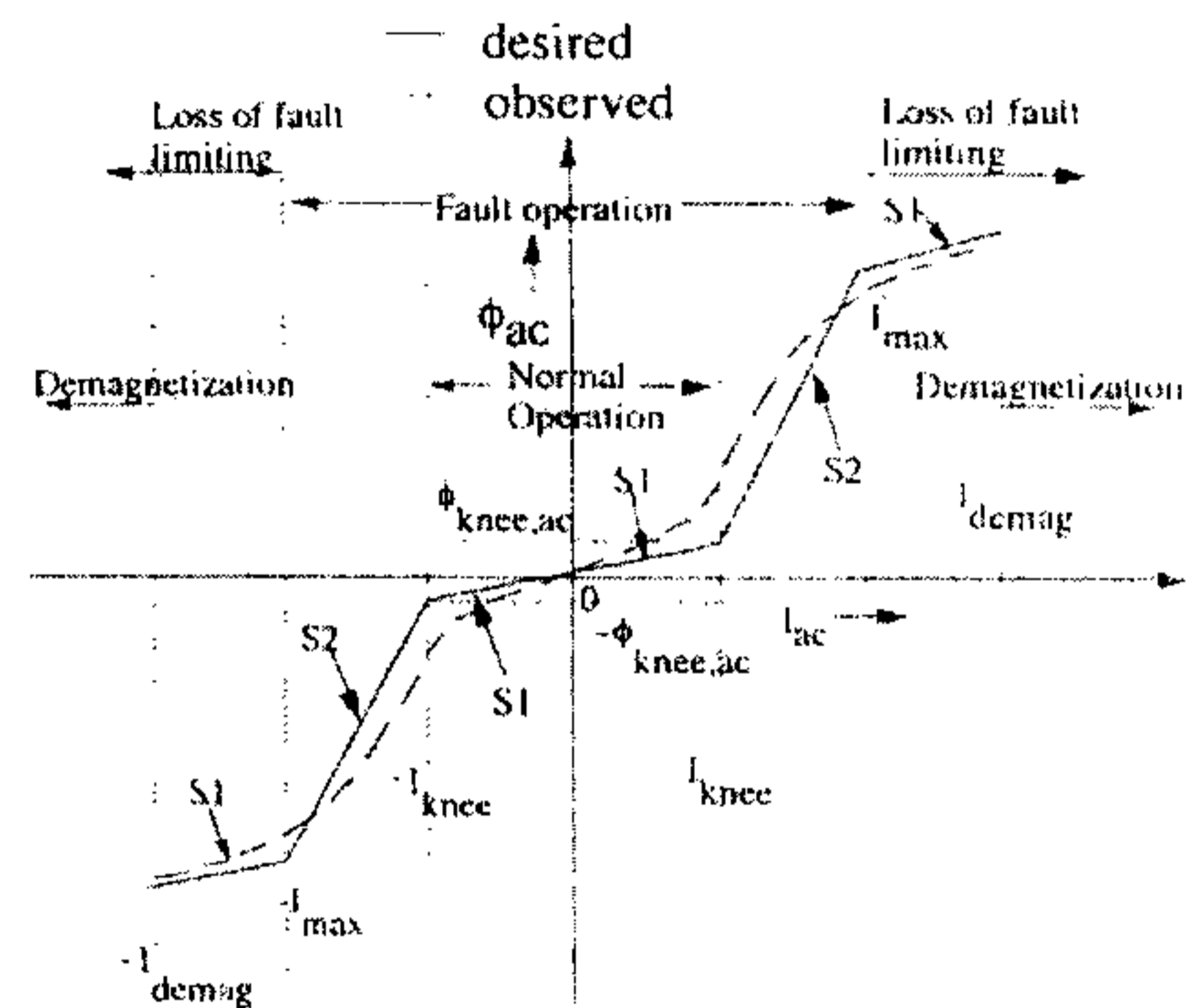

Fig. 2 B-H characteristics and operating point

Fig. 3 The φ-i characteristics of the complete system

Based on this above principle different types of magnetic current limiter have been fabricated and experiments were conducted. The magnetomotive force of the PM and the coil may act in series or in parallel. Fig. 4 shows a fabricated series biased limited based on ferrite core and permanent magnet made of Nd-Fe-B [1]. Fig. 5 shows a fabricated parallel biased limiter based on steel core and permanent magnet [2]. The models shown in Fig. 4 and 5 are used for single phase system. Fig. 6 shows a fabricated model for three-phase system based on ferrite core and ring type PM [3].
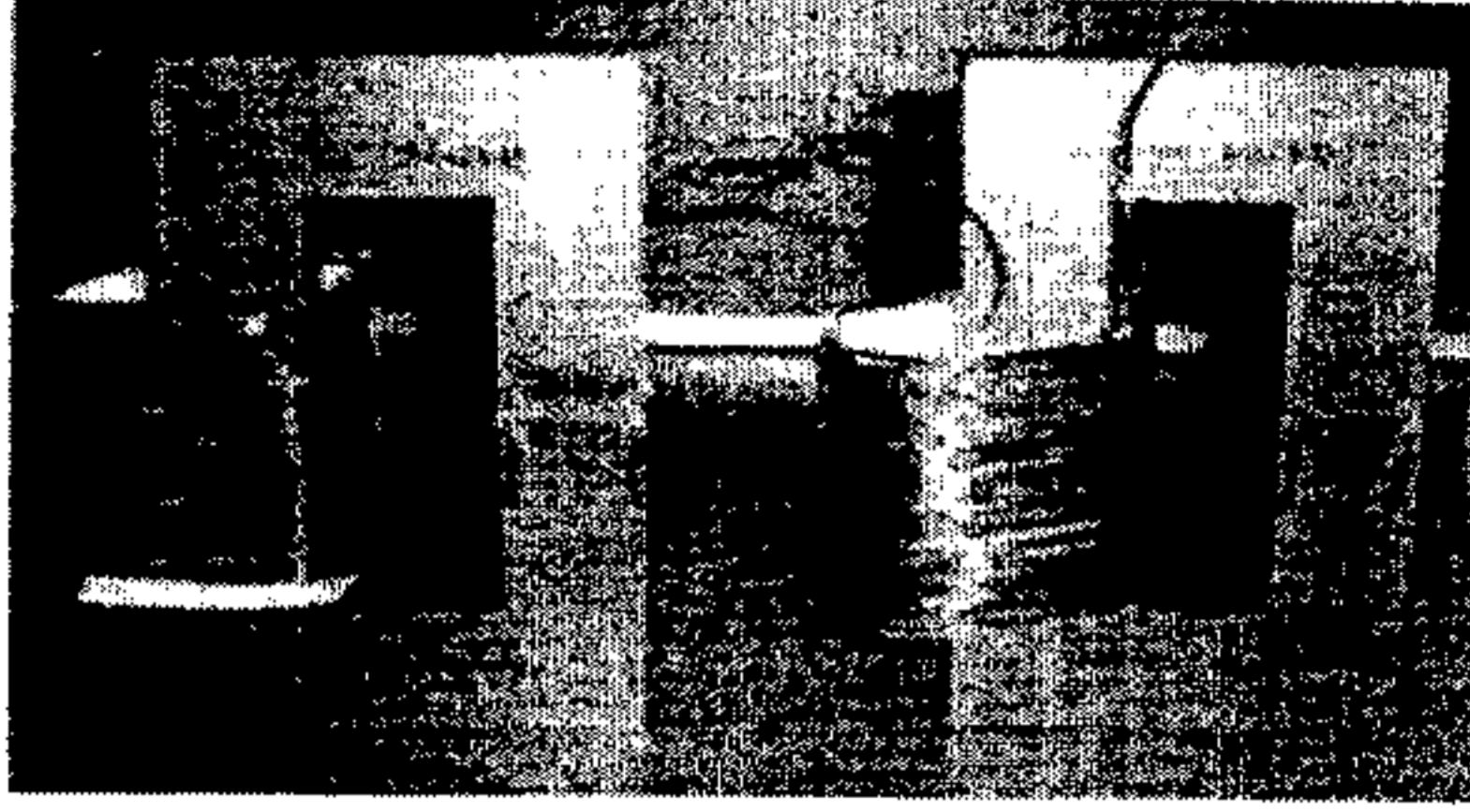

Fig.1 Basic structure of MCL

Fig. 4 Series biased MCL based on ferrite core and permanent magnet
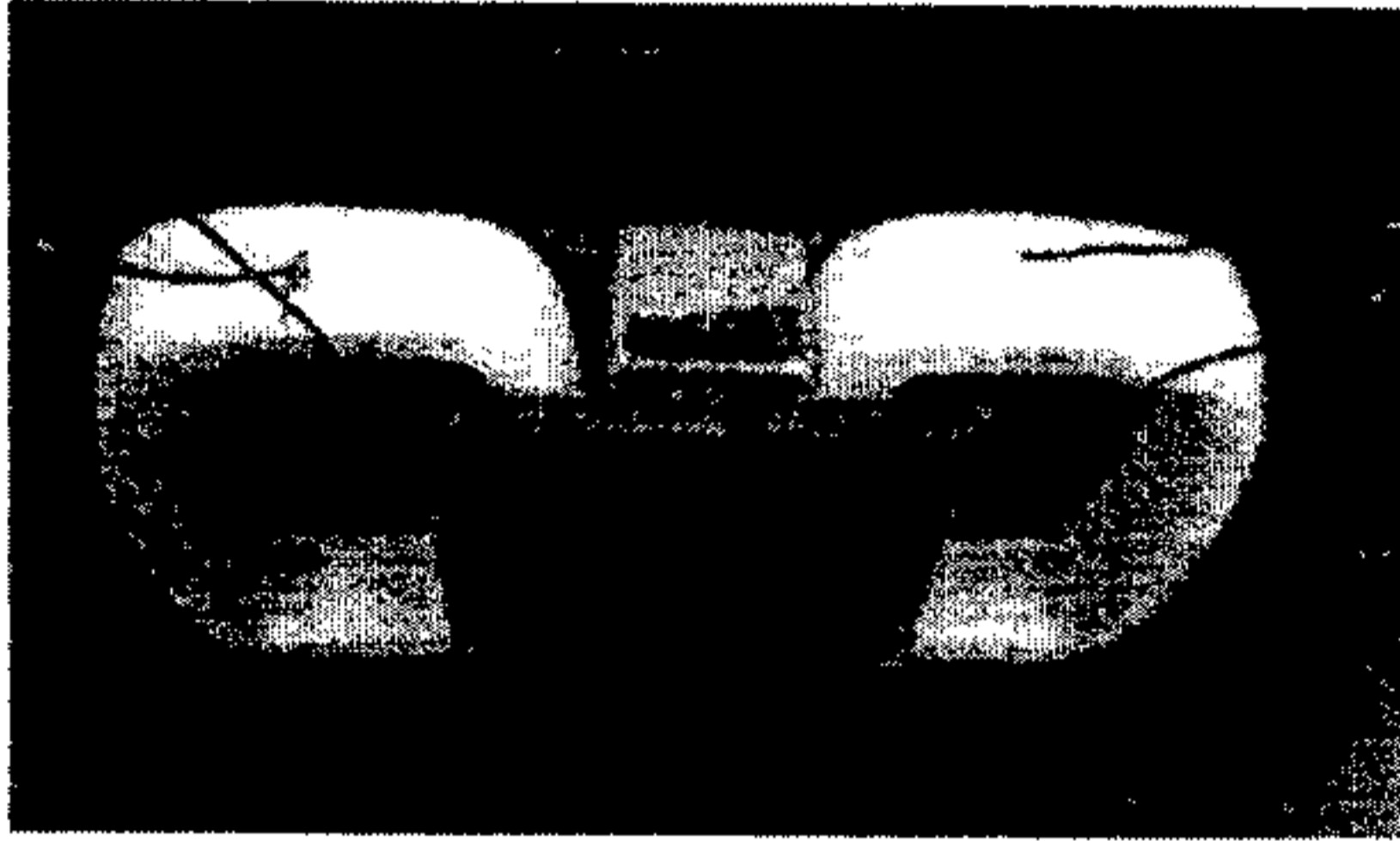

Fig. 5 Parallel biased MCL based on steel core and permanent magnet
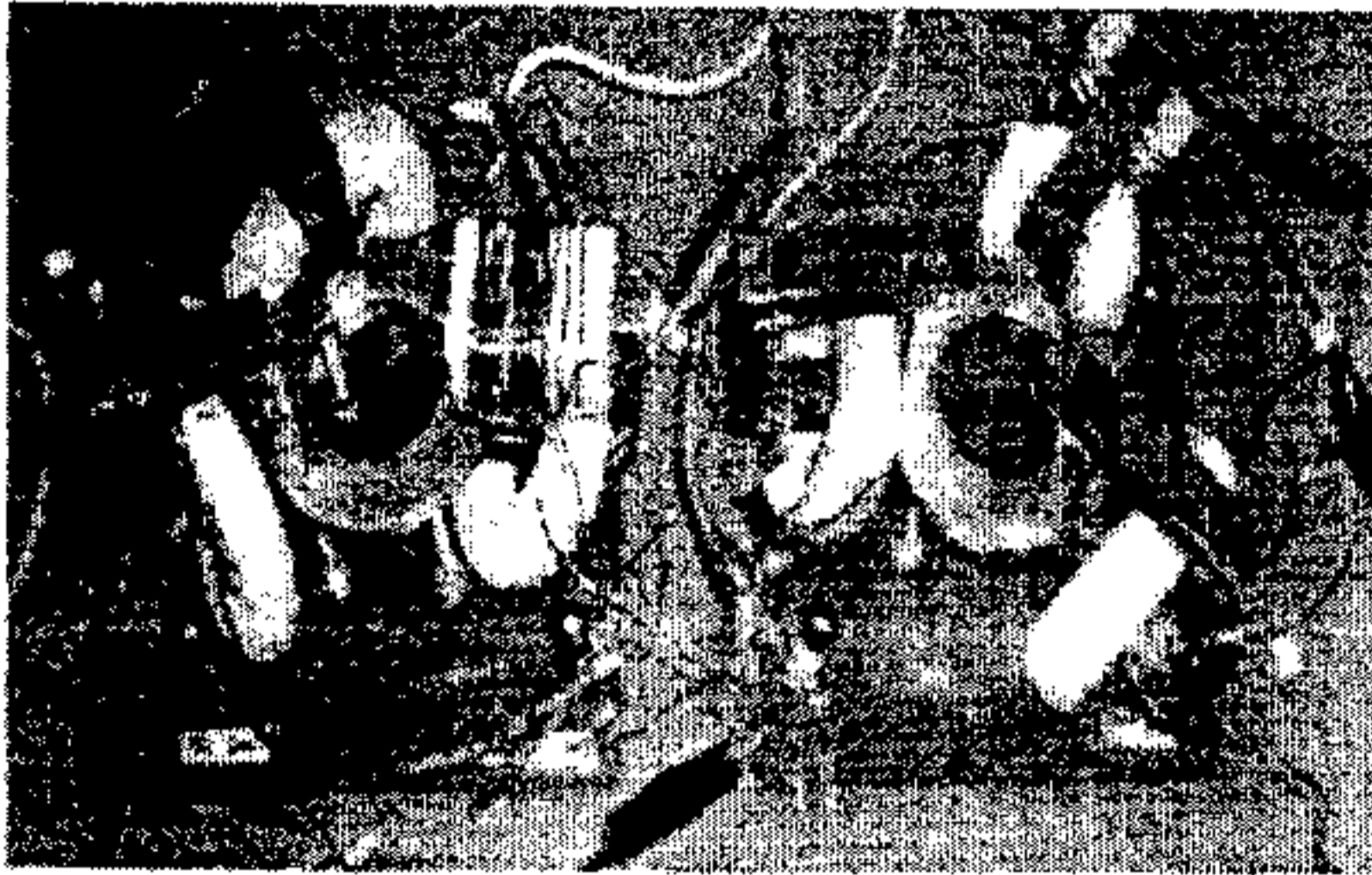

Fig. 6 Series biased MCL based on ferrite core and ring type permanent magnet for three-phase system

3. DESIGN CRITERION AND APPLICATION AREAS OF MCL

The basic design criterion of magnetic curent limiter is explained in this section. During the fault condition to avoid the PM to be in the loss of current limting and demagntization zone as shown in Fig. 3, the following condition is to be satisfied.

$$H_c l_m \geq N I_{max} \qquad (1)$$

where H_c is the coercive force of the PM and l_m is the length of the PM. I_{max} is the maximum current allowed during the fault condition. H_c is dictated by the PM itself and is not under designer's control. The minimum value of N, i.e. the turn of the coil may be 1. So the maximum value of current i.e. system level is dependent on the length of the magnet.

Under normal condition the voltage drop across the MCL is to be very low and is given by

$$V_{NOR} = X_s I = 2(2\pi f L_s)I = 4\pi f L_s I \qquad (2)$$

The voltage across the MCL during fault condition to be very large and is given by

$$V_{FAULT} = X_u I = 2\pi f (L_s + L_u)I \qquad (3)$$

where L_s and L_u are the saturated and unsaturated inductance respectively and are given by

$$L_s = \frac{N^2}{R_m + R_s} \quad \text{and} \quad L_u = \frac{N^2}{R_m + R_u} \qquad (4a, b)$$

where R_m, R_s and R_u are the reluctance of PM, saturated reluctance of the core and unsaturated reluctance of the core respectively and are given by

$$R_m = \frac{l_m}{\mu_m S}, \quad R_s = \frac{l_{core}}{\mu_s S} \quad \text{and} \quad R_u = \frac{l_{core}}{\mu_u S} \qquad (5a, b, c)$$

where S is the common area of the core or PM, μ_m, μ_s and μ_u are permeabilities of PM, saturated core and unsaturated core respectively.

Under fault condition the full voltage appears across the MCL. So we can write $V_{supply} = X_u I_{FAULT}$.

So the ratio of the normal voltage drop across MCL to the supply voltage is given by

$$\frac{V_{NOR}}{V_{supply}} = \frac{X_s I_{NOR}}{X_u I_{FAULT}} = \frac{1}{k}\frac{X_s}{X_u} = \frac{1}{k}\frac{2L_s}{L_s + L_u} = \frac{2}{k}\frac{1}{1 + L_u/L_s}$$

(6) ; k is the ratio of I_{FAULT} to I_{NOR}.

From (4a, b) and (5a, b, c) we can write

87

$$\frac{L_u}{L_s} = 1 + \frac{\mu_m}{\mu_s}\frac{l_{core}}{l_m} \quad (7)$$

the reluctance R_u is neglected with respect to R_m. For NdFeB PM, the permeability $\mu_m \approx 1.8\mu_0$ and assuming $l_{core}/l_m = 100$, we get

$$\frac{L_u}{L_s} = 1 + \frac{180}{\mu_{rs}} \quad (8)$$

μ_{rs} is the relative permeability of the core under saturated condition. The variation of the ratio L_u/L_s as a function of μ_{rs} is shown in Fig. 7. It is seen that a higher value of L_u/L_s demands a very low value of saturated permeability, μ_{rs} of the core. It is difficult to get core with that much low value of μ_{rs}. So with the available value of μ_{rs}, it is difficult o achieve a high value of L_u/L_s which means the voltage drop across the limiter under normal operating condition is quite large. So this type of limiter is suitable in power electronic based systems as shown in Figs. 8 and 9, in which the voltage across the load can be adjusted. Usually the magnetic current limiter are suitable for supply system of voltages up to 600 V and current up to a few hundreds of amperes. In Figs. 8 and 9 this type of limiter can be used to limit the fault during the failure of the power electronics devices such as transistors, diodes etc.
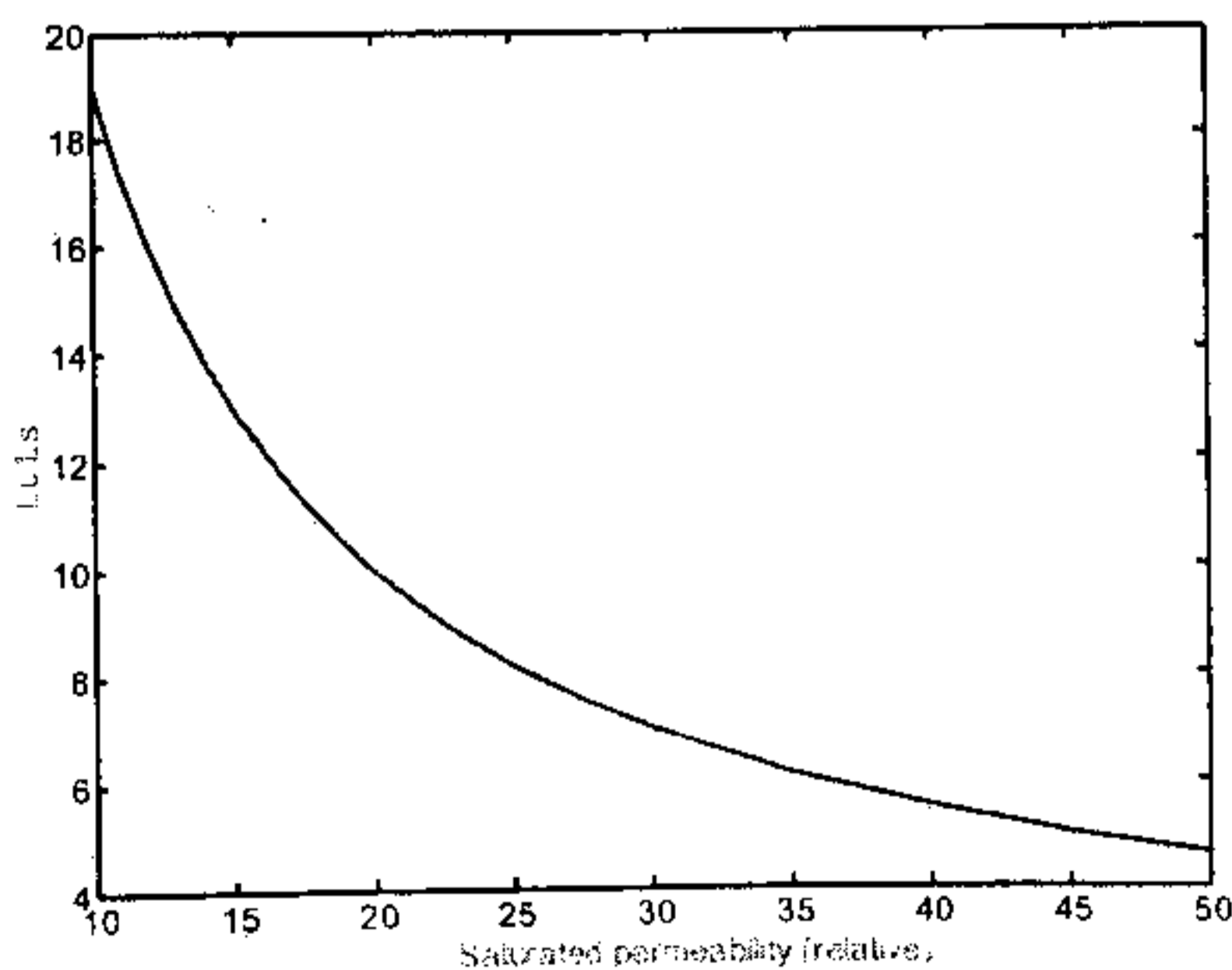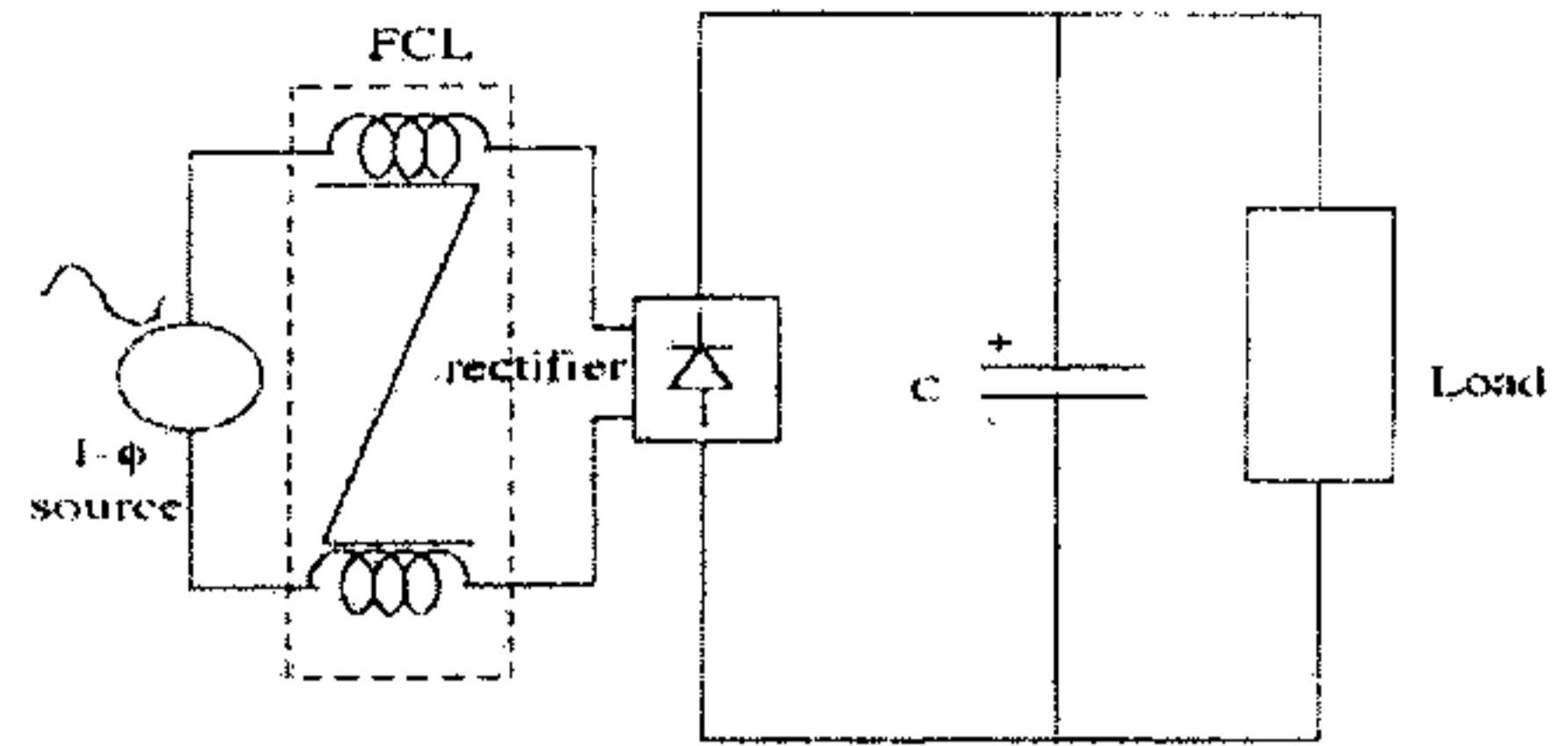

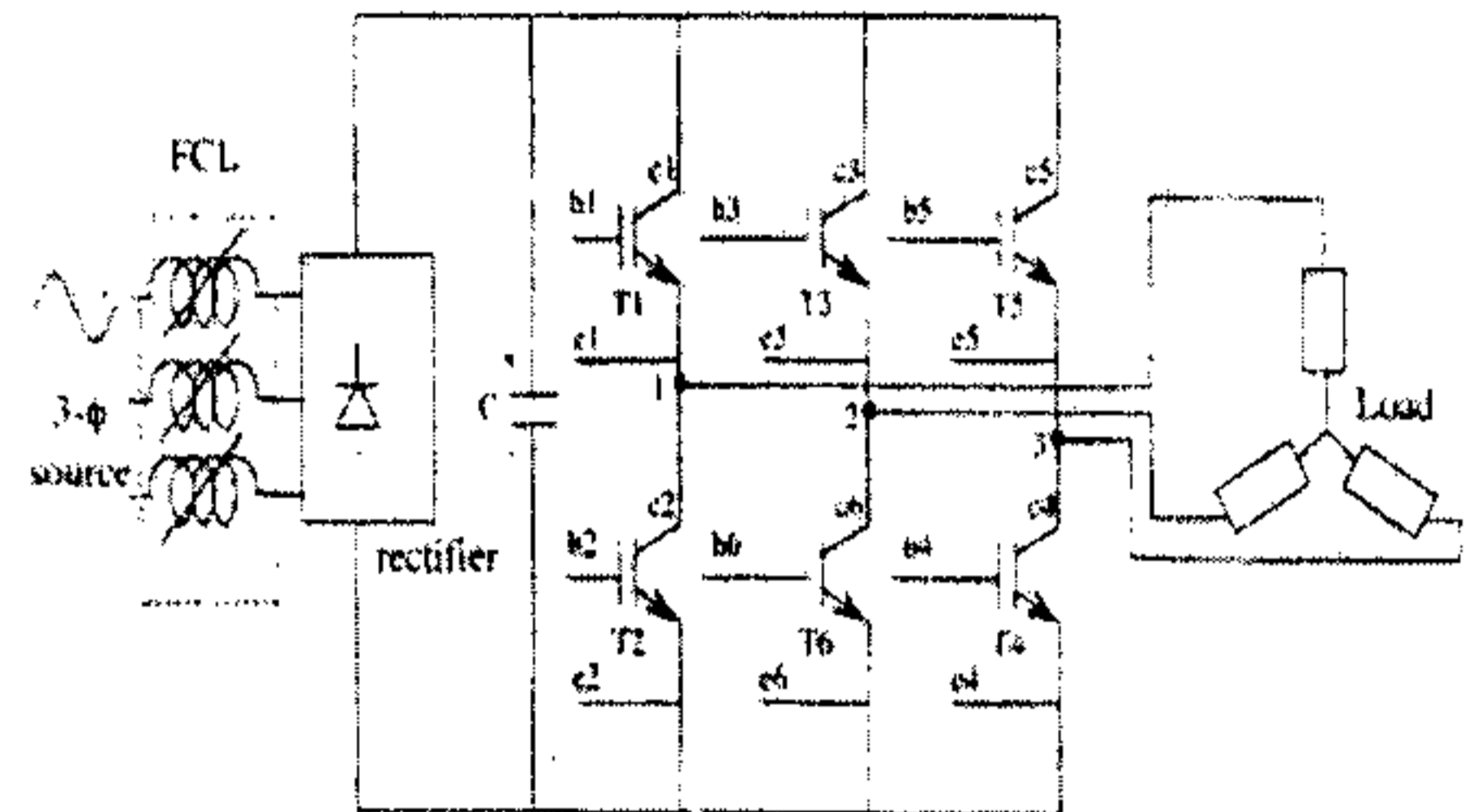Fig. 8 A typical single phase power electronic system for the application of MCL

Fig. 9 A typical three phase power electronic system for the application of MCL

Fig. 10 shows the starting line current with and without MCL for the circuit shown in Fig. 8 with a discharged capacitor. It is seen that in the absence of MCL the peak starting current reaches nearly 95 A. In contrast, the peak current with the MCL in place is 55 A. This is less that 200% of the nominal peak current.
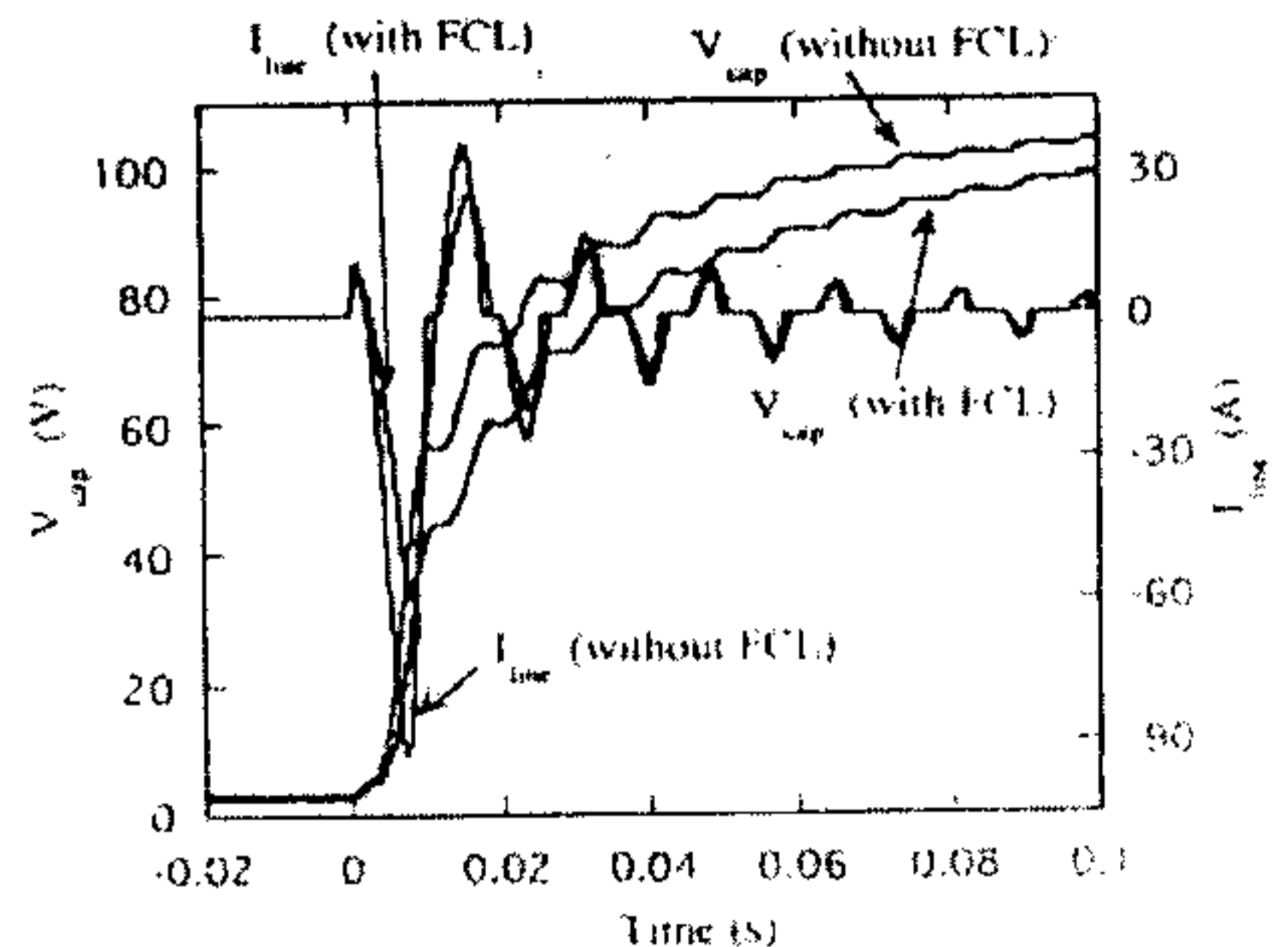

Fig. 7 The variation of L_u/L_s with μ_{rs}

Fig. 10 Starting current waveforms with and without MCL

88

Fig. 11 shows the current and voltage waveforms under a shorted diode condition. It is seen that the peak current is reduced considerably when the MCL is inserted.
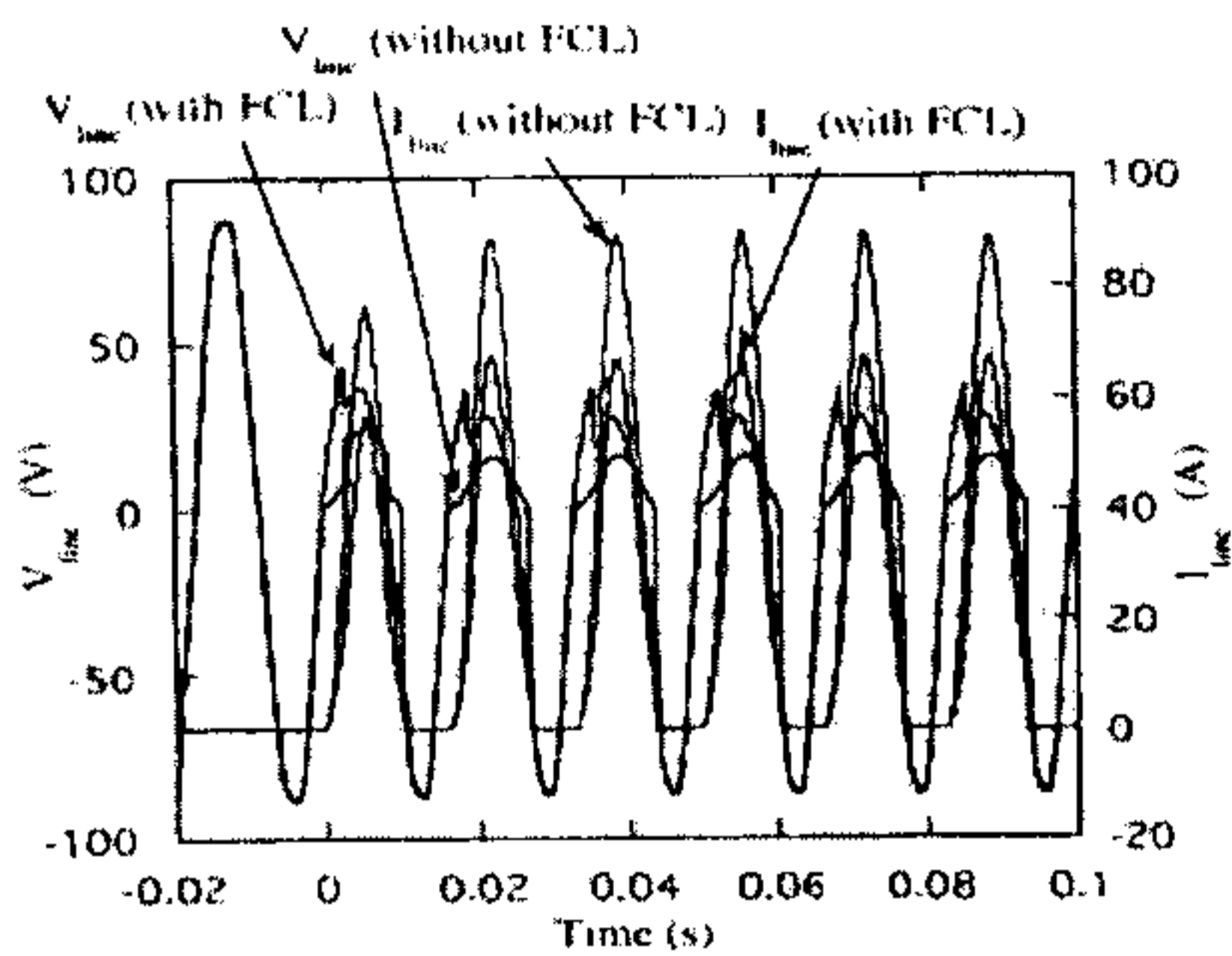

Fig. 11 Current waveforms under a shorted diode condition

Fig. 12 shows the line currents and voltage during shorted load condition. It is seen that the peak current is considerably less due to MCL.
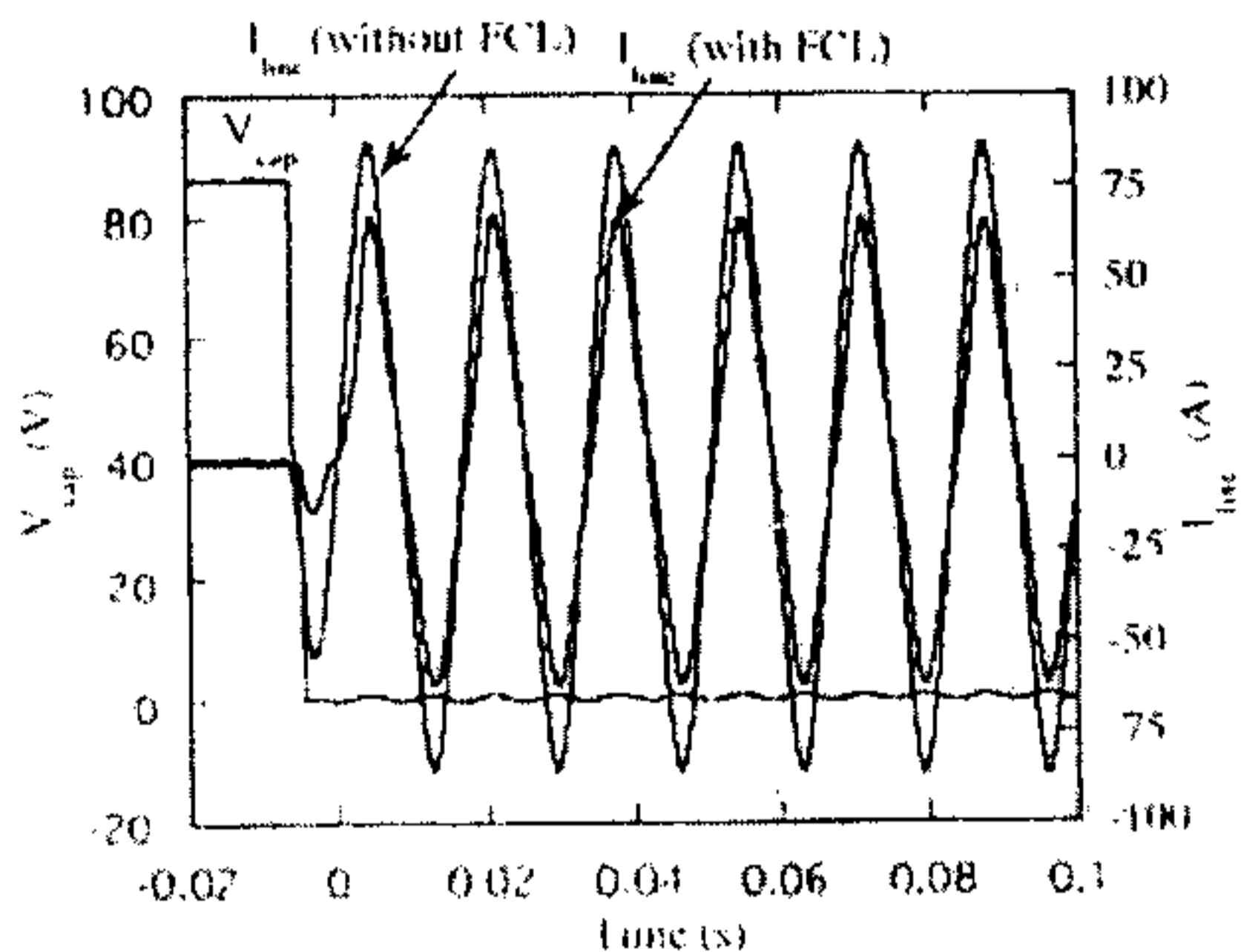

Fig. 12 Current waveforms under shorted output condition

4. TRANSITION TO HTSFCL

From the earlier discussion it has become very clear that the MCL cannot be used in all applications and not suitable for large system. In order to apply limiter for large capacity power system the use of high temperature superconducting fault current limiter (HTSFCL) [4] has been investigated with the use of computer modeling. The power companies here in New Zealand are reluctant to go for High Temperature Superconducting Fault Current Limiter (HTSFCL) to be introduced before they investigate the impact of HTSFCL on the existing power systems and economical aspect. They would like to simulate the short circuit studies to verify the impact on current levels due to the introduction of HTSFCL and also to investigate how a HTSFCL can enhance the performance of a power system. In order to do that an accurate circuit model of the FCL needs to be introduced in power system simulator. So the aim of this section is to derive a voltage-current characteristic i.e. a circuit model of the device with different operating parameters. A resistive type FCL has been considered for a typical 11 kV, 1 kA system. The novelty of the paper is the development of a transient thermal model to be used for the prediction of temperature distribution of the HTSFCL.

While designing and developing the HTSFCL the following points are considered.

(1) The V-I characteristic of the limiter from normal to fault state should give a large transition of resistance to limit the fault current.

(2) The voltage drop during normal condition should be very less, typically less than 1% is desirable.

(3) Since during the fault condition full voltage appear across the limiter, there will be considerable amount of power loss in the case of resistive type limiter. The power loss will increase the temperature. A detailed thermal model is required to get a very clear picture. In order to get the recovery of the

superconducting properties, the heat should be removed as early as possible.

(4) The soldering of the superconductor wire with the normal wire may introduce the contact drop/resistance.

Based on the above discussion the following aspects are to be looked into.

(1) Material aspects – to find the best among $Bi_2Sr_2CaCu_2O_{8+\square}$ (Bi2212), $Bi_2Sr_2Ca_2Cu_3O_{10+y}$ (Bi2223) and $YBa_2Cu_3O_{6+z}$ (Y123). We have the expertise of developing these materials.

(2) Limitation behavior, (3) Limitation time, (4) Recovery time, (5) Losses, (6) Overload capability

(7) Transient behavior – inrush current, (8) Power quality, (9) Coupling of Grids, (10) Connection of power stations, (11) Protection of auxiliary devices.

5. ANALYSIS OF HTSFCL

A meander patterned HTS wire has been considered to configure FCL. Fig. 13 shows a schematic model along the cross-section of the FCL. The model has been discretized with many non-overlapping nodes.

The general non-steady thermal equation is known to be $K\nabla^2 T + q^* = C\dfrac{\partial T}{\partial t}$ (9); K is the thermal conductivity, q* is the internal generated heat per unit volume, and C is the specific heat. The heat q* is given by

q* = E.J ; where E is the electric field intensity and J is the current density of the HTS wire. The calculation of E and J are discussed in the next section.

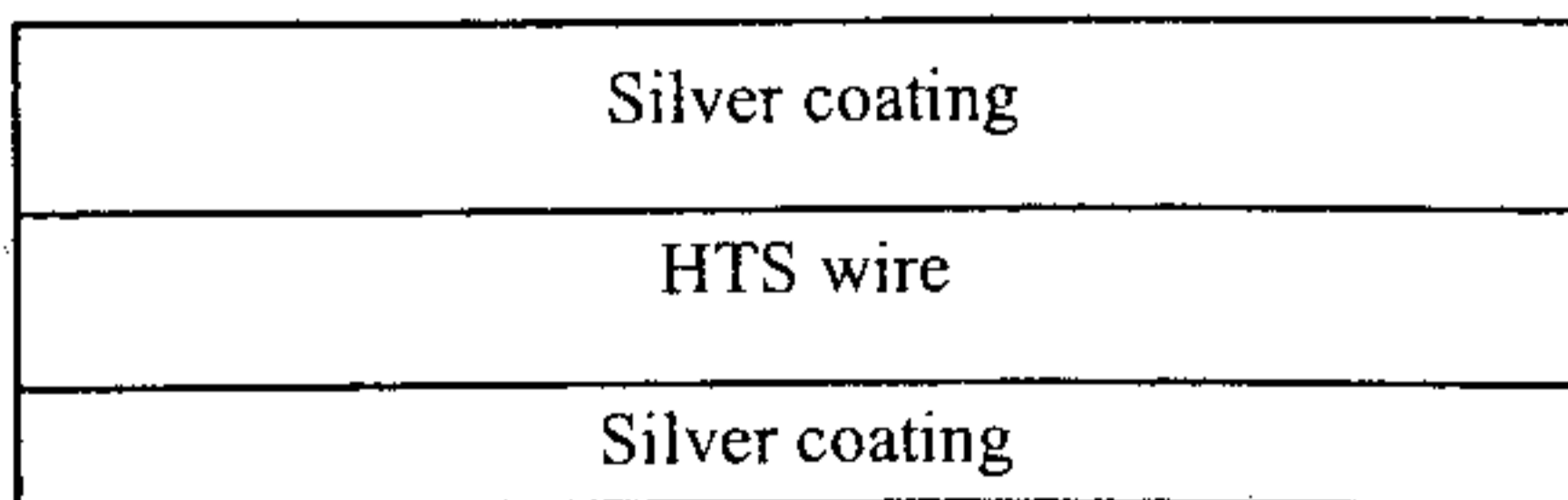| Silver coating |
|---|
| HTS wire |
| Silver coating |

Fig. 13 Schematic of FCL for analysis

The steps of analysis of HTSFCL are divided into two states : (i) Normal condition and (ii) Fault condition. The relationship between the current density and the electric field intensity for both the conditions are discussed below.

Normal condition: In normal condition the current is decided by the external circuit parameters i.e., the load impedance. The current density, J, for the HTS wire is thus calculated dividing the current by the area. The electric field intensity of the HTS wire is thus given by [5]

$E = E_o(\dfrac{J}{J_{c77}})^{b1}$ (10); E_o = 1E-4 and b1 = 20.

The voltage across the HTS wire is thus obtained by multiplying the electric field intensity with the length.

Once the electric field intensity, E is obtained, the heat loss, E.J, is calculated. The temperature, T using the heat loss, is calculated based on the developed thermal model.

Fault condition: During the fault condition the full voltage appears across the FCL. So the electric field intensity is decided by the supply voltage and the length of the HTS wire. The current density of the HTS wire is a function of the operating temperature and the electric field intensity.

The temperature dependence of the critical current density is expressed as [5]

$$\dfrac{J_c(T)}{J_c(T=0)} = (1-\dfrac{T}{T_c})^x$$ (11)

T_c and x for different HTS materials are given by

Ag/Bi-2223: T_c = 105-110 K   x = 1.4
Ag/Bi-2212: T_c = 85-92 K   x = 1.8
Y-123: T_c = 88 K   x = 1.2

Based on the operation at 77 K with liquid nitrogen the current density during fault condition is given by

$$J = J_{c77}(\dfrac{T_c-T}{T_c-77})^x(\dfrac{E}{E_o})^{1/b1}$$ (12)

The current density of each node is thus calculated and the current of each section is obtained multiplying the corresponding area associated with each node. The total current is calculated by taking the sum of all the current along the cross-section of the HTS wire.

Fig. 14 shows the temperature distribution along the depth of the HTS wire for different values of electric field intensity. The higher value of E will produce higher temperature rise but the required length of wire will be shorter and consequently reduction in cost. Fig. 15 shows a current vs time characteristics for a typical fault condition with different values of E. It is seen that the fault current becomes larger with the large values of E. Fig. 16 shows the variation of temperature with time for different values of E.
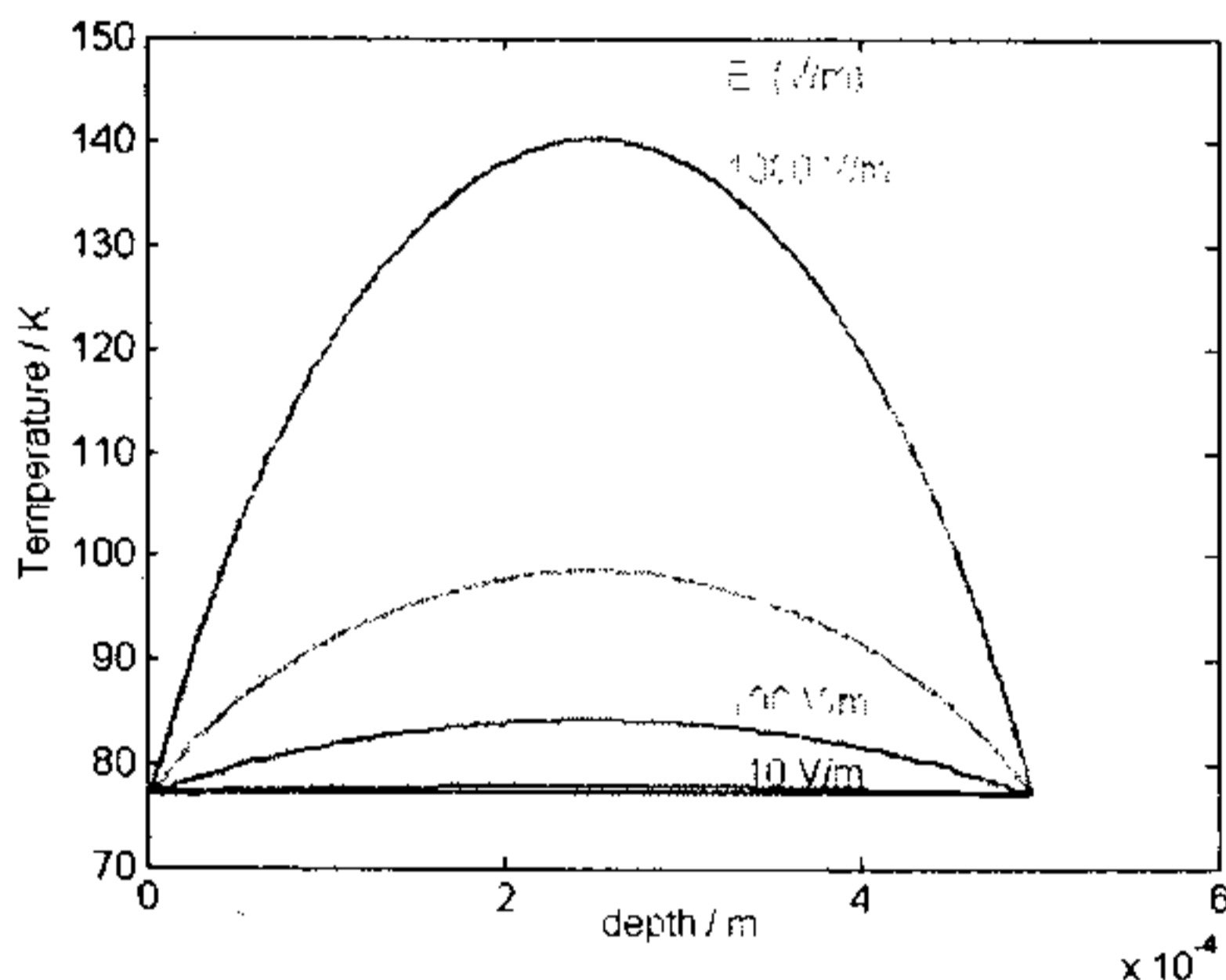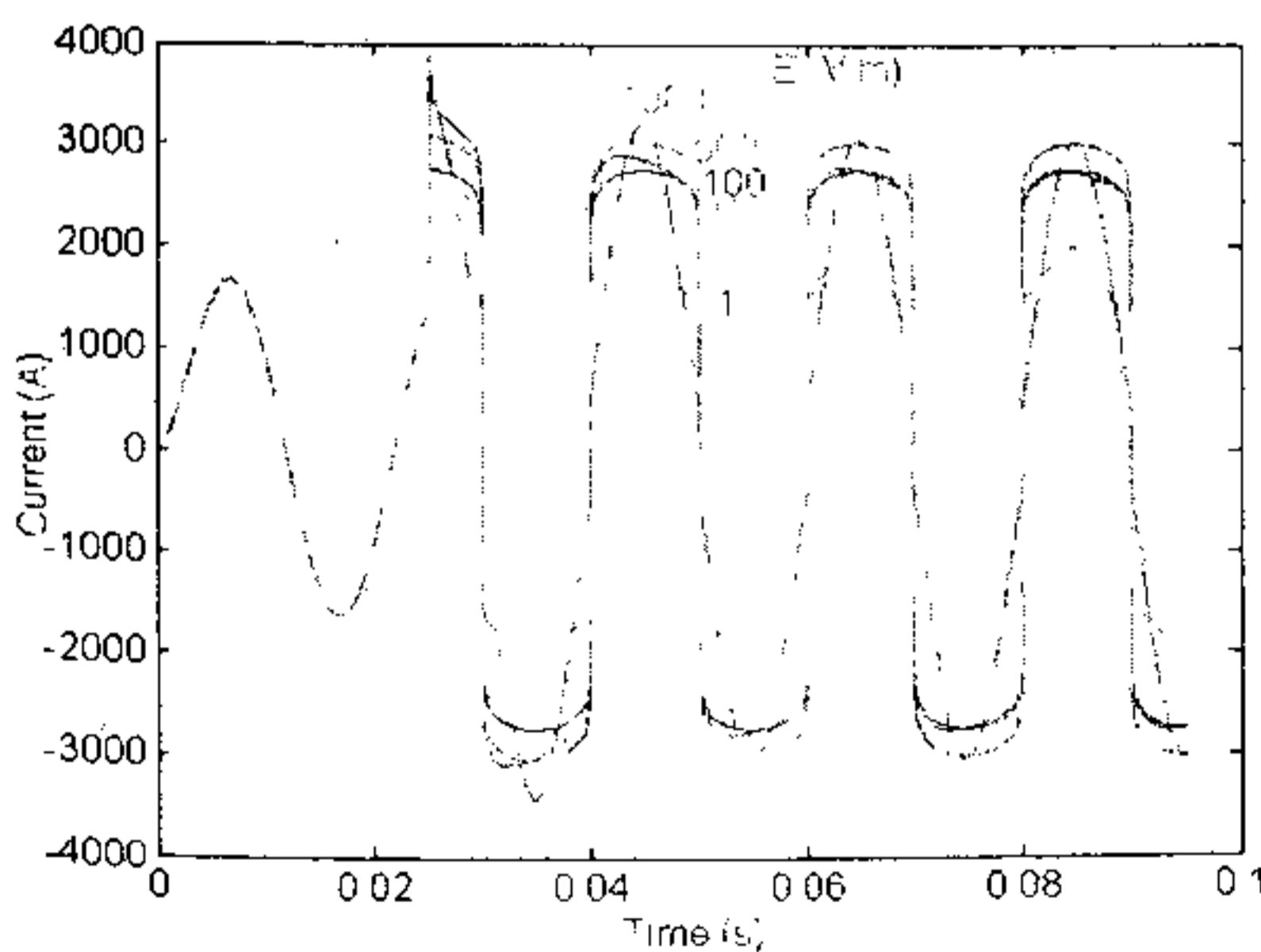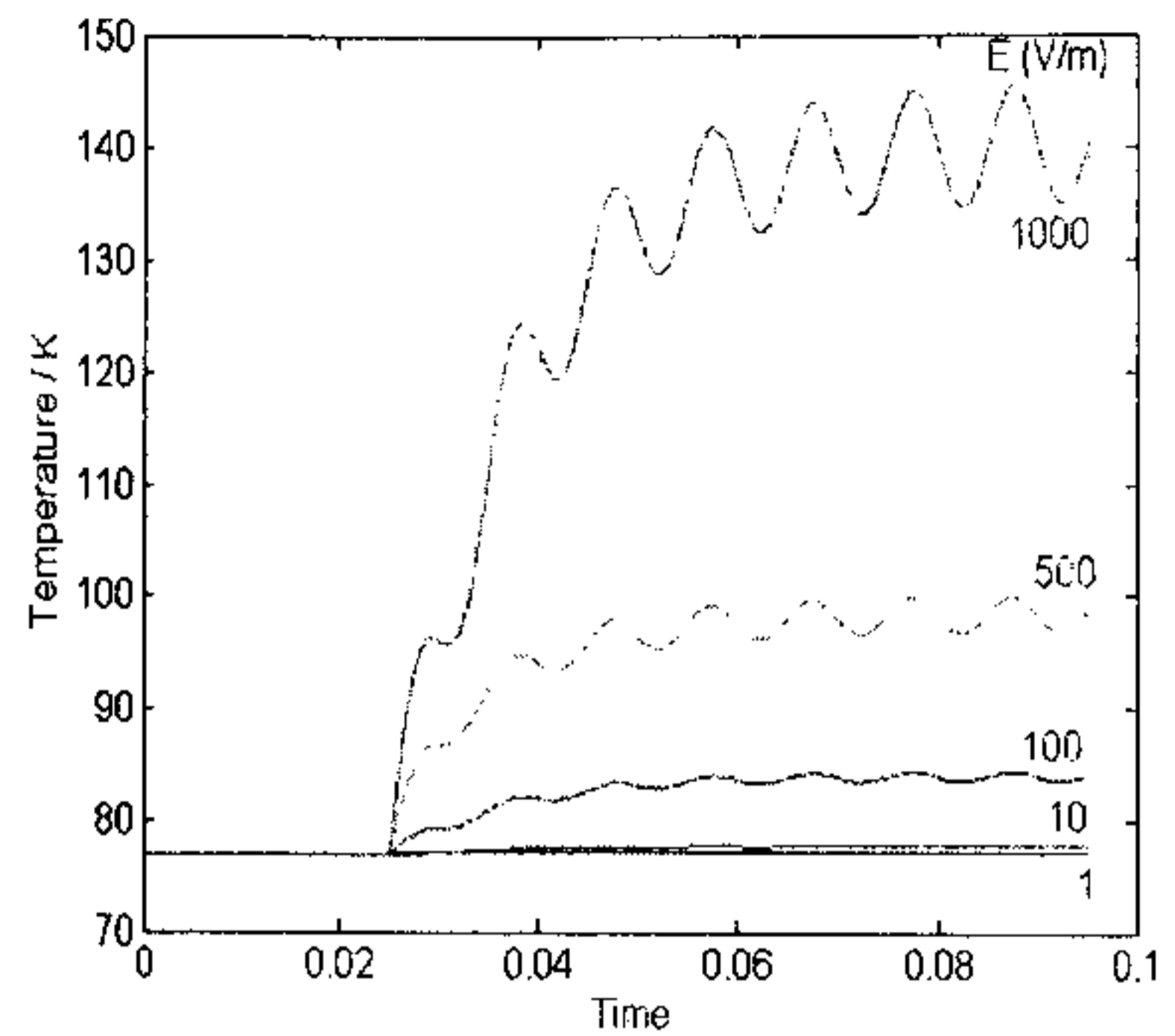

Fig. 16   Temperature vs time characteristic

Fig. 17 shows the variation of current with time for different values of critical current density, J_c. It is seen that the HTS material with higher J_c allows larger fault current to flow. The higher values of J_c will allow less cross-sectional area of the HTS material.

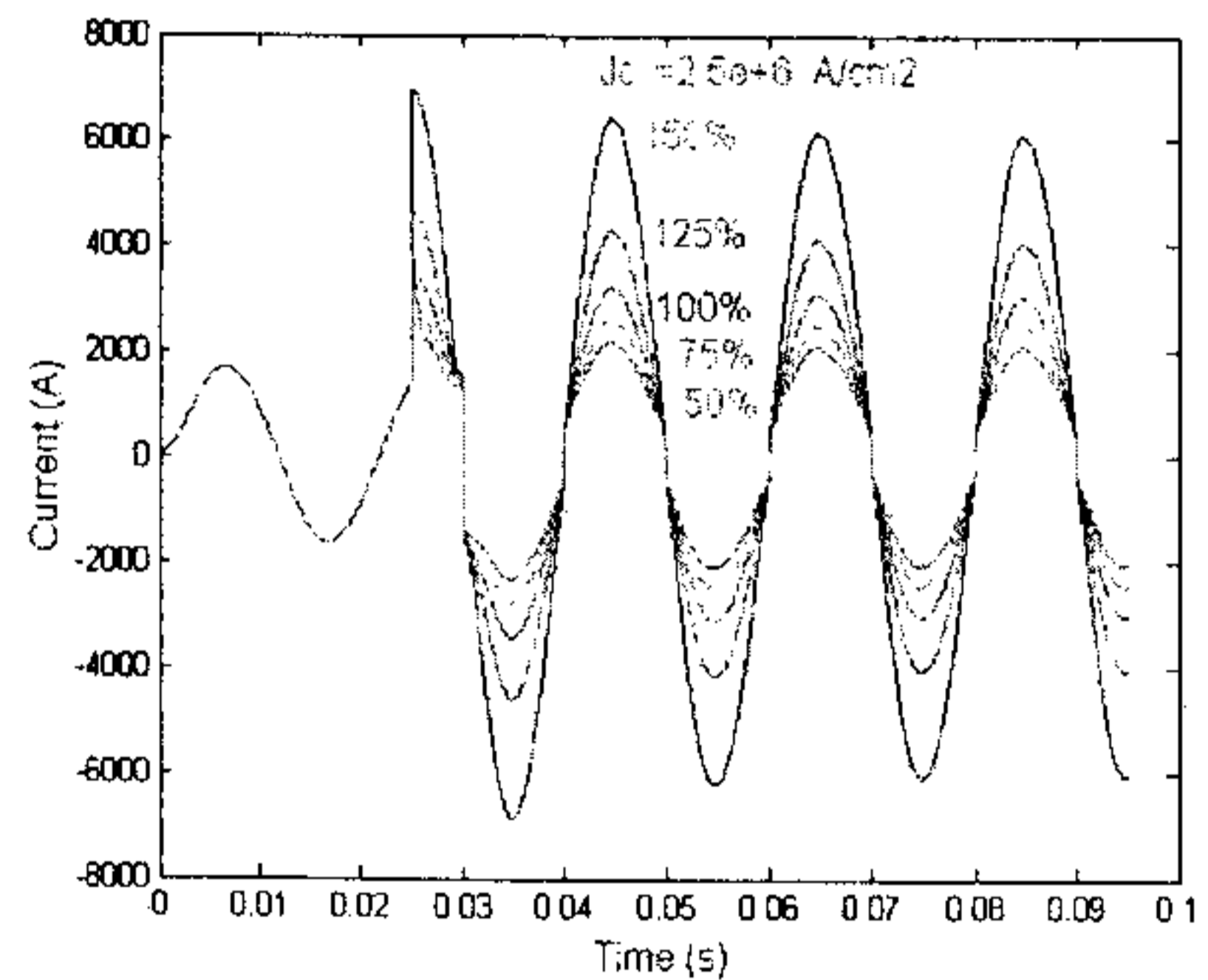Fig. 14   Temperature distribution along the depth for various E's

Fig. 17 Variation of fault current with time for different values of Jc

Fig. 18 shows the final value of temperature almost 4 cycles after fault with different values of depth of the limiter. It is seen that the final value of temperature is higher for larger value of depth of the HTS wire. A lot of other conditions have been simulated.
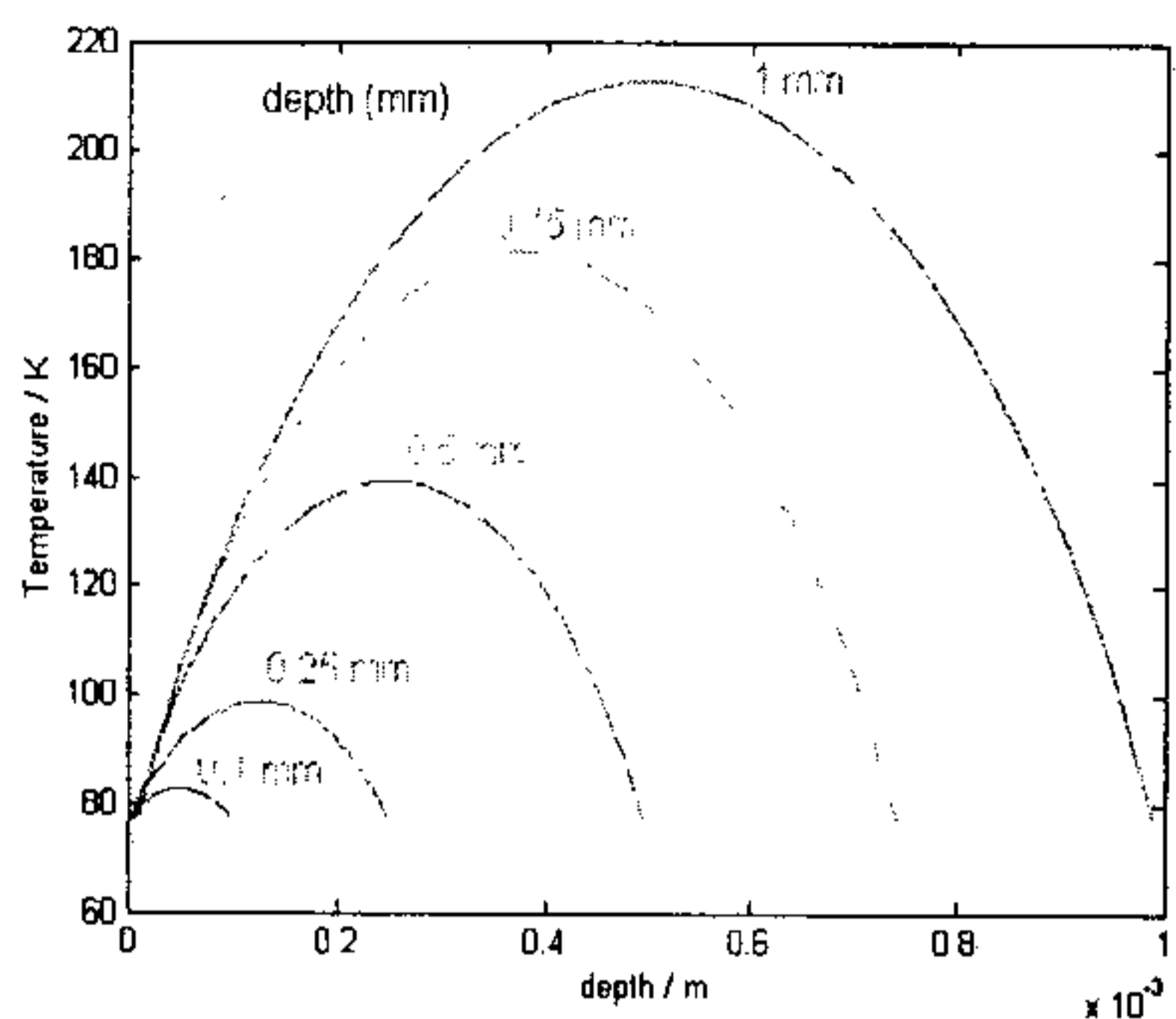

Fig. 15   Current vs time characteristics

91

Fig. 18 Variation of fault current with time for depth

6. CONCLUSIONS

This paper have described the basic design philosophy of two types of fault current limiter. A comprehensive analysis of HTSFCL has been carried out, the results of which will be very useful to New Zealand electric power generation and transmission companies. A novel thermal model has been developed for the prediction of transient thermal performance of high temperature superconducting fault current limiter. The dependent of fault current and temperature rise for varying operating parameters are obtained from this model. This model can be used to design the FCL for a sample system and the critical optimum parameters for overall good transient performance.

REFERENCES

[1] S.C.Mukhopadhyay, M.Iwahara, S.Yamada and F.P.Dawson, " Analysis, design and experimental results for a passive current limiting device", IEE proceeding on Electric Power Applications, vol. 146, no. 3, pp. 309-316, May 1999.

[2] M.Iwahara, S.C.Mukhopadhyay, S.Yamada and F.P.Dawson, "Development of passive fault current limiter in parallel biasing mode", IEEE transc. on Magnetics, Vol. 35, No. 5, pp 3523-3525, September 1999.

[3] S.C.Mukhopadhyay, F.P.Dawson, M.Iwahara and S.Yamada, "A novel compact magnetic current limiter for three phase applications", IEEE transc. on Magnetics, Vol. 36, No. 5, pp. 3568-3570, September 2000.

[4] W.Paul, et.al., "Test of 1.2 MVA high-Tc superconducting fault current limiter", Proc. On Superconducting Sci. Technol., IOP Publishing Ltd., 10 (1997), 914-918.

[5] G.E.Marsh and A.M.Wolsky, "AC losses in high-temperature superconductors and the importance of these losses to the future use of HTS in the power sector", Report submitted to International Energy Agency, USA, May 2000.